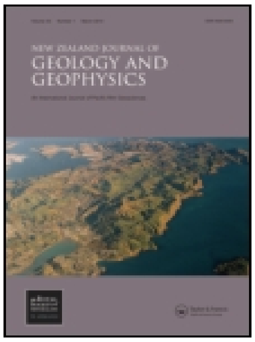

Taylor & Francis
Taylor & Francis Group

New Zealand Journal of Geology and Geophysics

ISSN: 0028-8306 (Print) 1175-8791 (Online) Journal homepage: http://www.tandfonline.com/loi/tnzg20

Evolution of the 2010–2012 Canterbury earthquake sequence

S Bannister & K Gledhill

New Zealand Journal of Geology and Geophysics
Vol. 55, No. 3, September 2012, 295–304

Taylor & Francis
Taylor & Francis Group

Evolution of the 2010–2012 Canterbury earthquake sequence

S Bannister* and K Gledhill

GNS Science, Lower Hutt, New Zealand

(*Received 16 December 2011; final version received 11 March 2012*)

We present an overview of the evolution of the 2010–2012 Canterbury earthquake sequence, summarising the findings from a broad range of studies on the larger earthquakes. The sequence began with the M_W7.1 Darfield earthquake on 4 September 2010 and continued in a series of aftershocks through the remainder of 2010 and early 2011, before the devastating M_W6.2 Christchurch earthquake of 22 February 2011 which resulted in 185 deaths, more than NZ$11 billion of damage and extensive liquefaction. Another significant M_W6.0 aftershock occurred on 13 June 2011 causing more liquefaction and damage in the eastern hill suburbs, while further activity, including events of M_W5.8 and M_W5.9, occurred offshore from Christchurch in December 2011. Only the Darfield earthquake resulted in visible surface faulting, with a c. 30-km-long east–west-trending surface rupture exhibiting horizontal displacements of up to 5 m. The earthquakes displayed a variety of strike-slip and reverse faulting mechanisms. The entire Canterbury earthquake sequence has been well recorded by an extensive permanent seismograph network (GeoNet) and additional temporary instruments, providing a rare set of near-source recordings of high ground accelerations and broadband waveforms that will influence earthquake studies in New Zealand and overseas for decades to come.

Keywords: Canterbury earthquakes; Darfield earthquake; Christchurch earthquake; high stress drop; complex rupture; aftershocks; Greendale Fault; New Zealand GeoNet

Introduction

The M_W7.1[1] Darfield earthquake and the subsequent Canterbury 2010–2012 earthquake sequence have produced more than 8700 earthquakes larger than M_L2, with a diverse mixture of strike slip and reverse faulting occurring on previously unknown faults (Sibson et al. 2011). The earthquakes in this sequence have had a devastating effect on Christchurch, and the surrounding Canterbury region. The seismicity has been well-recorded by the GeoNet network (Gledhill et al. 2011), and by temporarily deployed seismometers, providing rare, densely spaced, near-fault data for future research. Here we summarise the evolution of the Canterbury earthquake sequence up to the end of January 2012.

4 September 2010 Darfield earthquake

The M_W7.1 Darfield earthquake occurred on 4 September 2010 at 04:35 NZST (3 September at 16:35 UTC) c. 40 km west of Christchurch, on previously unknown faults beneath the Canterbury Plains (Figs 1–3). The earthquake caused extensive damage in Christchurch city, and left a well-defined 29.5-km-long surface rupture, striking east–west in its central portion, c. 4 km south of the epicentre, that has subsequently been named the Greendale Fault (Fig. 1; Van Dissen et al. 2011; Quigley et al. 2012). The surface rupture is characterised by a series of left-stepping fault traces with a maximum step-over of 950 m (Quigley et al. 2012; Villamor et al. 2012). Surface displacement on the Greendale Fault was predominantly right-lateral strike slip, with an average horizontal displacement of c. 2.5 m and maximum displacements of c. 5 m horizontally and c. 1.5 m vertically, as measured at the surface (Quigley et al. 2010).

Seismological, GPS and processed satellite (InSAR) information all suggest that the earthquake rupture was a complex process involving rupture of multiple fault segments (Beavan et al. 2010; Holden et al. 2011; Beavan et al. 2012). Results from the inversion of strong motion wavefor data (Holden et al. 2011) suggest that the earthquake initiated on a blind thrust fault, termed the Charing Cross Fault (Fig. 1), c. 6 km to the north of the Greendale Fault trace, with the initial rupture progressing to the southwest from the hypocentre to the intersection with the Greendale Fault. This interpretation is supported by the GeoNet moment tensor solution (Fig. 1), as well as geodetic modelling (J Beavan et al. 2012). Although the aftershock pattern does not fully support this interpretation, the aftershocks of complex thrust ruptures often do not show clear alignment with fault structures at depth (e.g., Abercrombie et al. 2000). Gledhill et al. (2011) noted that the USGS centroid moment tensor solution is a

[1]Moment magnitudes are those derived from moment tensor inversion using New Zealand local and regional stations (Ristau 2008), as recorded in the online New Zealand GeoNet moment tensor database (GeoNet 2011a).

*Corresponding author. Email: s.bannister@gns.cri.nz

ISSN 0028-8306 print/ISSN 1175-8791 online

http://dx.doi.org/10.1080/00288306.2012.680475
http://www.tandfonline.com

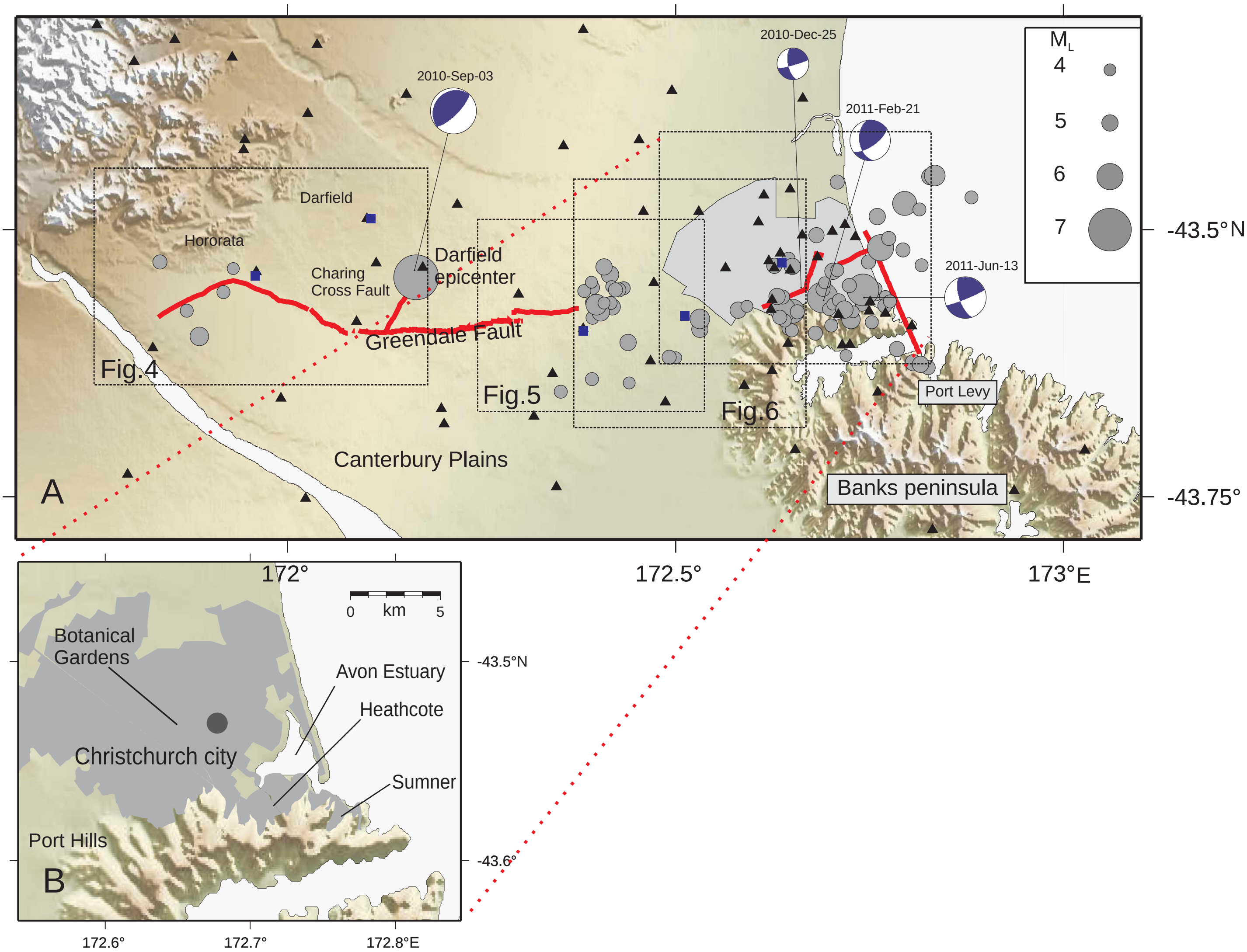

Figure 1 Setting of the Canterbury earthquake sequence. **A**, Location of events greater than M_L4.5, together with the inferred location of the Greendale Fault (dark solid line), Charing Cross Fault (dark solid line), and fault segments associated with the 22 February 2010 and 13 June 2010 earthquakes. Moment tensor solutions are shown for the Darfield mainshock, and three other large earthquakes (details in Table 1), as documented by GeoNet using local and regional stations. **B**, Expanded map of Christchurch city.

strike-slip solution, whereas the GeoNet moment tensor solution is pure thrust. They suggested that the data from the local and regional stations used for the GeoNet solution better captured the higher frequency signal associated with the first few seconds of rupture on the Charing Cross Fault; the first motion measurements support this interpretation.

The Darfield earthquake rupture appears to have then ruptured both east and west along the Greendale Fault, but predominantly eastward (Holden et al. 2011). Both geodetic (Beavan et al. 2010; Beavan et al. 2012) and seismological models (Holden et al. 2011) indicate that most of the displacement was very shallow, and was mainly confined to the upper c. 5 km. Fault models developed from the inversion of InSAR measurements indicate slip on some of the fault segments reached 8 m at 4 km depth, indicating large stress drops of c. 10 MPa (Elliott et al. 2012), while aftershock relocations by Syracuse et al. (2012) along the central Greendale Fault segment indicate event depths from 5.9 to 14 km, mainly several kilometres below the regions of highest slip inferred by Beavan et al. (2010).

The westward-propagating rupture on the Greendale Fault is inferred to have triggered slip on an intersecting blind thrust fault near Hororata, at the western end of the Greendale Fault (Holden et al. 2010), as indicated by both geodetic modelling (Beavan et al. 2010) and strong-motion modelling (Holden et al. 2011). Relocated aftershocks for the region around the Horotata fault (Fig. 4), derived using double-difference tomography (Zhang & Thurber 2003) confirm the presence of seismic activity on a steeply northwest-dipping plane, closely matching the parameters

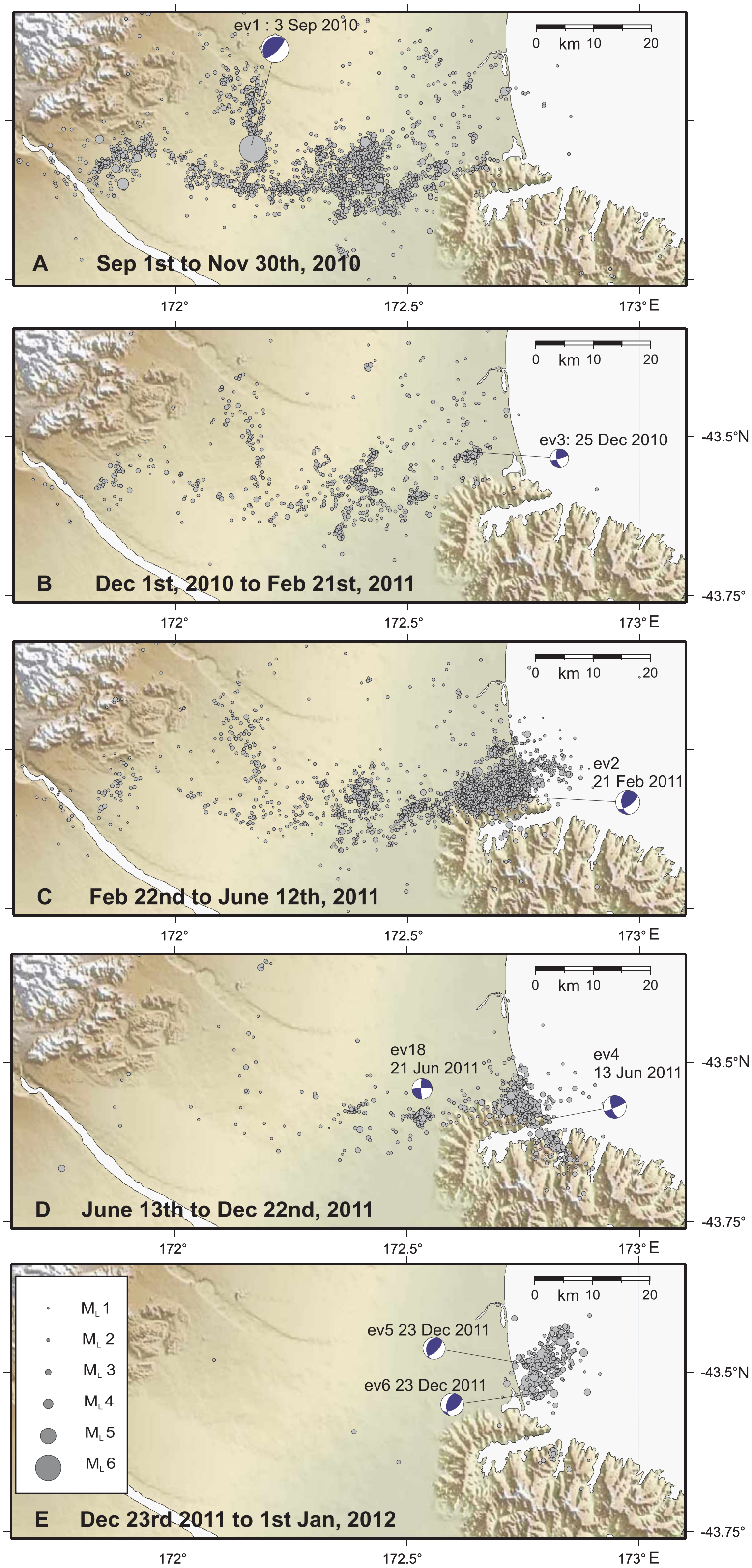

Figure 2 Relocated epicentres for earthquakes are shown for the following periods. **A**, 1 September to 30 November 2010. **B**, 1 December 2010 to 21 February 2011. **C**, 22 February to 12 June 2011. **D**, 13 June to 22 December 2011. **E**, Between 23 December 2011 and 1 January 2012. Earthquake symbol size varies exponentially with the local magnitude M_L.

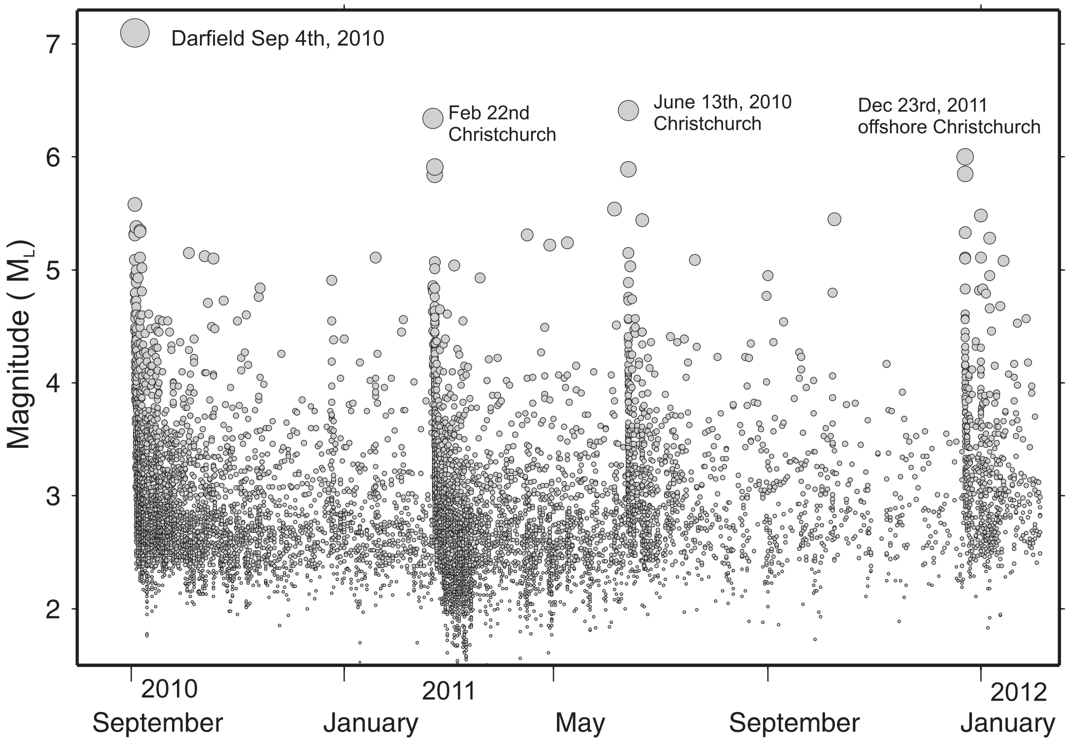

Figure 3 Time sequence of the 2010–2012 Canterbury earthquakes, for all earthquakes located by GeoNet in the Canterbury region between September 2010 and February 2012, plotted as a function of local magnitude (M_L).

found from moment tensor solutions (Ristau 2008; GeoNet 2011a; Sibson et al. 2011) for some of the larger aftershocks in the vicinity.

The eastward-propagating rupture on the Greendale Fault continued for at least c. 20 km to within a few kilometres of Rolleston, as indicated by the surface deformation

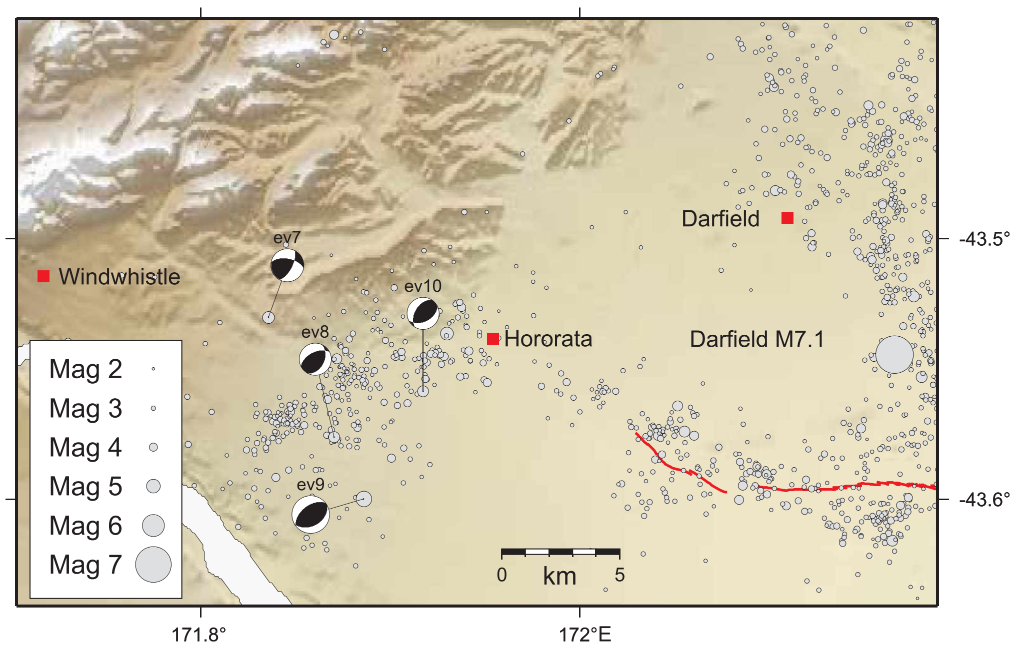

Figure 4 Aftershock epicentres after relocation analysis, highlighting the blind thrust fault at Hororata. Earthquake symbol size varies exponentially with the local magnitude M_L. This fault is thought to have triggered as part of the complex Darfield rupture (Holden et al. 2011), reaching a maximum slip of 2.8 m at c. 1 km depth. Reverse fault mechanisms shown are GeoNet moment tensor solutions for three of the larger events (event labels refer to event number in Table 1).

(Quigley et al. 2010; Van Dissen et al. 2011) and implied by kinematic inversion (Holden et al. 2011) and geodetic inversion results (Beavan et al. 2012). The presence of a subsidiary right-lateral fault extending to the northeast has also been inferred (Beavan et al. 2010; Beavan et al. 2012) and, tentatively, a fault segment striking east–southeast from near the eastern end of the Greendale Fault (Beavan et al. 2012). Relocated aftershock locations for events in the first few weeks after the Darfield mainshock, indicate an aftershock cluster with a northwest–southeast trend near Rolleston (Fig. 5), at the easternmost end of the Greendale surface trace. This suggests that the Greendale Fault rupture terminated at an intersection with a previously unknown blind sinistral fault, which then became active over the following 1–2 weeks. However, the subsequent high level of activity in the vicinity of Rolleston and Lincoln over the ensuing months, as shown in Fig. 6, is distributed and complex, with a mixture of strike-slip and normal-faulting mechanisms (Gledhill et al. 2011; Sibson et al. 2011), and so details of the fault structure in the area around Rolleston are difficult to ascertain.

More than 7300 felt reports were lodged with GeoNet following the Darfield earthquake, including over 100 reports of Modified Mercalli Intensity (MM) 8 and some reports of MM9. The highest felt intensities were in the epicentral region, but also extended east to Christchurch. Recorded ground acceleration reached 1.26 *g* at the Greendale seismic station, and up to 0.3 *g* in central Christchurch, > 35 km from the epicentre. Long-period ground motions in central Christchurch had peaks at c. 2.5 s that exceeded design spectra; these peaks can be attributed to amplification effects from the deep sedimentary basin beneath Christchurch (Webb et al. 2011), but also suggest the existence of a long-period component to the earthquake source signature (Cousins & McVerry 2010). Liquefaction effects were widespread in many eastern areas in the Canterbury Plains, including Christchurch city's eastern and southwestern suburbs and the town of Kaiapoi, c. 17 km north of Christchurch city centre (Orense et al. 2011).

Aftershock activity between 4 September 2010 and February 2011

Following the Darfield earthquake, and up to February 2011, more than 4300 aftershocks with local magnitudes of up to M_L5.4 were recorded by the GeoNet seismograph network. The aftershock activity was initially particularly concentrated at the eastern end of the Greendale Fault (Gledhill et al. 2011), and included eight events > M_L5 (Figs 1, 2), although these events did not cause significant damage to Christchurch city. Aftershock activity near the central and western segments of the Greendale Fault diminished quickly (Figs 2, 3).

Four months after the Darfield mainshock, on 25 December 2010 at 21:30 (UTC), an M_W4.7 aftershock

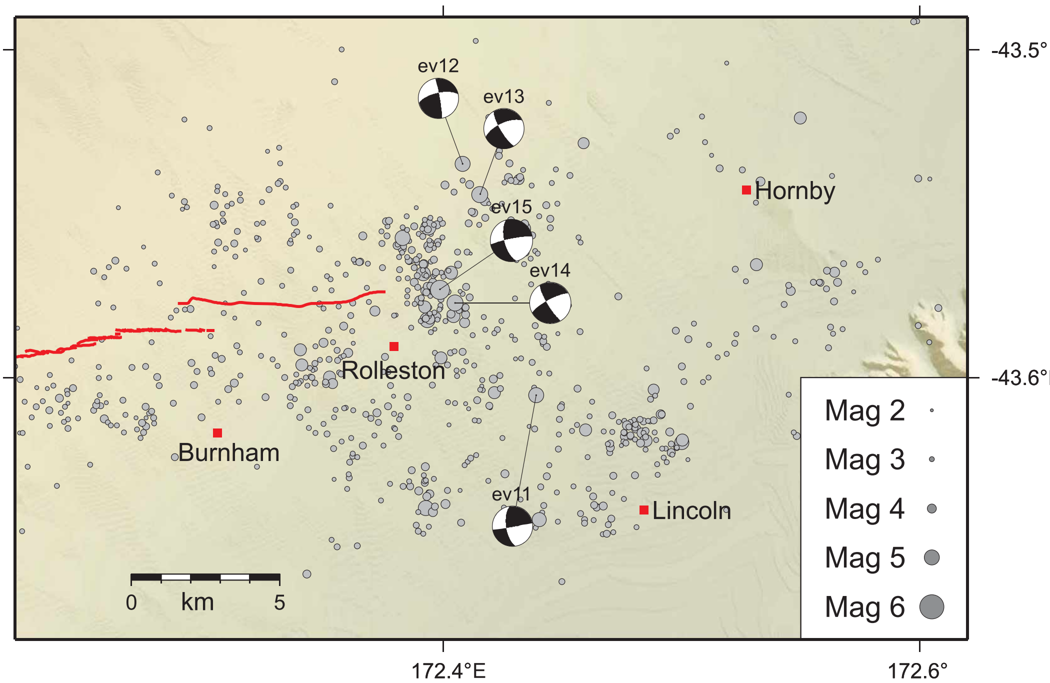

Figure 5 Epicentres of relocated earthquakes occurring between 4 and 30 September 2010, at the eastern end of the Greendale surface rupture (dark line). Earthquake symbol size varies exponentially with the local magnitude M_L. The spatial distribution of the epi centres suggest the presence of a northwest–southeast trending sinistral fault which may have played a role in terminating the Darfield rupture. GeoNet moment tensor solutions are shown for five of the larger events close to the inferred fault. Event labels refer to event number in Table 1. Seismic activity later migrated northeast and southeast from the Greendale Fault end.

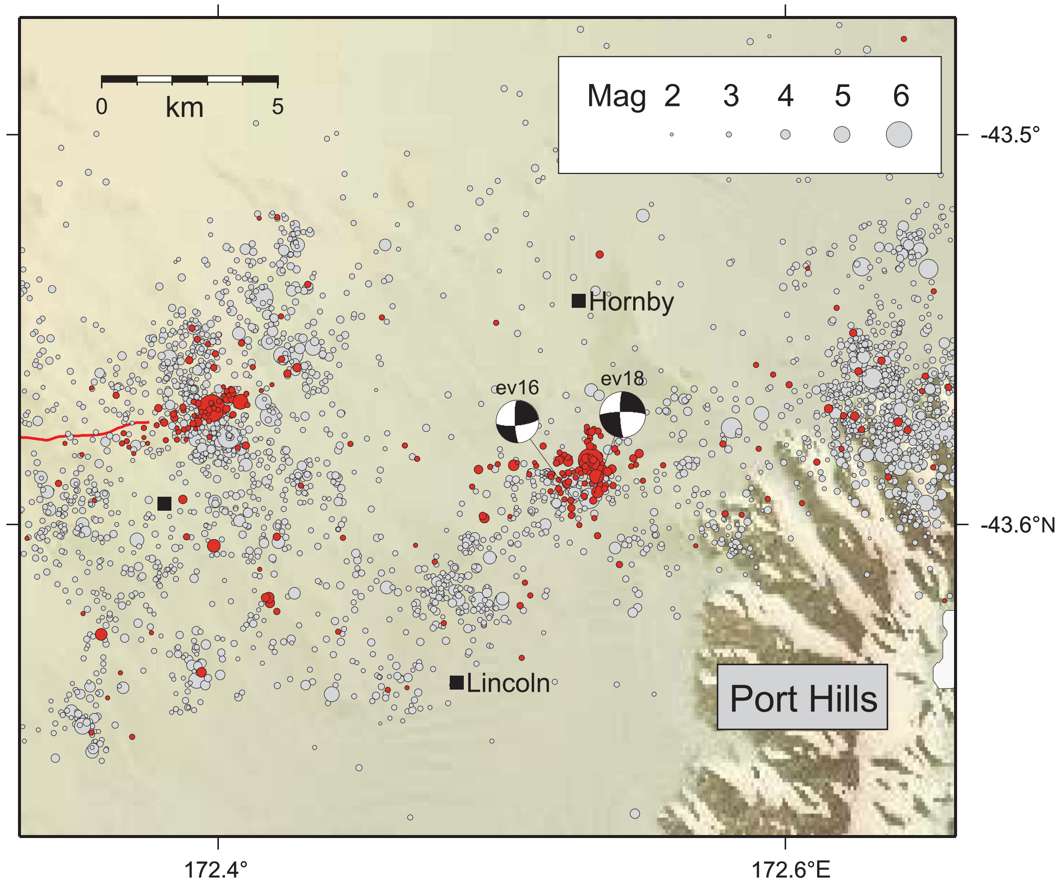

Figure 6 Aftershock epicentre locations for the area north of Lincoln, up to the end of June 2011. Earthquakes occurring before June 2011 are shaded light grey; those in June 2010 or later are infilled dark. Earthquake symbol size varies exponentially with the local magnitude M_L. There has been continued activity in the Lincoln–Prebbleton area since October 2010, with increased activity especially in June 2011, following the 13 June 2011 M_W6.0 earthquake. GeoNet moment tensor solutions are shown for two of larger events, suggesting north–northwest–south–southeast sinistral faulting for the cluster south of Hornby. Event labels refer to event numbers in Table 1.

occurred <2 km from Christchurch city centre (Figs 1, 2, Table 1), involving right-lateral strike slip (Bannister 2011). The earthquake caused significant damage in the city centre, with maximum peak ground acceleration of up to 0.4 *g* measured at the Christchurch Botanical Gardens (Fig. 1), and >0.2 *g* elsewhere in the city (Webb et al. 2011). There were 23 felt reports of MM7 shaking. This earthquake was accompanied by a short sequence of earthquakes over the next few hours, the largest two being M_L4.6 and M_L4.4 (Webb et al. 2011), and then by more than 30 events in close proximity over the next 3–4 weeks. Relocation analysis, using seismic wavefield cross-correlation estimates, indicate that the initial M_W4.7 earthquake was located at c. 4.0 km depth, with an epicentre 1.8 km northwest of the Christchurch city centre (Bannister 2011), while most of the subsequent events occurred at depths of between 3.5 and 7 km in a single patch <1 km^2 in area, with epicentres c. 1 km northeast of the city centre. The depth distribution of the aftershocks is consistent with a steeply dipping fault plane striking at c. 74°.

22 February 2011 Christchurch earthquake

The M_W6.2 22 February earthquake occurred at 12:51 NZDT (21 February 2011, 23:51 UT; Table 1), with an epicentre c. 6 km southeast of the Christchurch city centre (Fry et al. 2011a), five and half months after the Darfield earthquake (Fig. 2). Severe ground shaking was experienced in Christchurch city (Fry et al. 2011a,b) leading to extensive building damage, widespread liquefaction (Cubrinovski et al. 2011; Orense et al. 2011; Kaiser et al. 2011), landslides (Dellow et al. 2011), at least NZ$11 billion worth of building damage, and 185 fatalities. Ground motions reached 2.2 *g* in the Heathcote Valley near the epicentre and up to 0.8 *g* in the central business district (GeoNet waveform database in GeoNet, 2011c; Webb et al. 2011). Near-source peak horizontal accelerations (at distances less than c. 5 km from the fault) were in fact stronger in the Christchurch event than for the Darfield earthquake (Cousins & McVerry 2010; Kaiser et al. 2011).

Initial inversions of geodetic data (Beavan et al. 2010) and strong motion data (Holden 2011) suggested that the

Table 1 Hypocentre parameters for specific events discussed in the text and/or shown in Figs 3–5.

Event no.	CUSP-ID	Date/Time (UT)	Latitude (°N)	Longitude (°E)	Depth (km)	Moment Magnitude (M_W)
1	3366146	03/09/10 16:35	−43.539	172.156	9.9	7.2
2	3468575	21/02/11 23:51	−43.571	172.683	6.3	6.2
3	3437105	25/12/10 21:30	−43.541	172.625	5.3	4.7
4	3528839	13/06/11 02:20	−43.561	172.740	7.1	6.0
5	3631359	23/12/11 17:57	−43.537	172.783	7.8	5.8
6	3631380	23/12/11 23:36	−43.617	172.822	5.8	5.9
7	3366544	04/09/10 10:32	−43.378	171.835	21.1	4.3
8	3367278	05/09/10 17:07	−43.603	172.346	9.6	4.2
9	3367749	06/09/10 12:51	−43.537	172.330	12.6	5.0
10	3367765	06/09/10 13:39	−43.582	172.420	9.8	4.2
11	3366230	03/09/10 20:15	−43.630	172.395	9.7	4.8
12	3367742	06/09/10 12:41	−43.571	171.929	9.6	4.8
13	3382676	04/10/11 9:21	−43.547	172.408	9.1	4.8
14	3509905	09/05/11 15:04	−43.584	172.401	11.7	4.9
15	3525264	05/06/11 21:09	−43.576	172.396	9.3	5.1
16	3450113	19/01/11 17:03	−43.600	172.538	7.0	4.8
17	3468797	22/02/11 08:21	−43.589	172.581	7.7	4.3
18	3533107	21/06/11 10:34	−43.590	172.528	9.6	5.2

Note: CUSP-ID numbers refer to the event IDs in the GeoNet seismic event database. M_w values from GeoNet moment tensor database (GeoNet, 2011a). Locations are following double-difference relocation analysis.

fault rupture involved slip on a northeast–southwest striking fault plane dipping c. 70° to the southeast, with slip on the fault extending upwards to within c. 1 km of the surface beneath the Heathcote–Avon estuary and maximum slip of 2.5–4 m at 4–5 km depth. However Beavan et al. (2012) suggest that the geodetic and Light Detection and Ranging (LiDAR) data are better modelled with three fault segments, including a north–northeast-striking reverse fault segment. This more complex interpretation is in better accord with the distribution of relocated aftershocks (Bannister et al. 2011) which, north of the Port Hills, do not reveal a simple fault structure. No surface expressions have yet been found for these postulated faults: LiDAR data (Beavan et al. 2011) suggest that slip propagated almost to the surface, although it is unclear whether all of the fault slip was coseismic.

As summarised by Kaiser et al. (2011), a number of factors are thought to have contributed to the high accelerations experienced in Christchurch city during the 22 February event (Fry et al. 2011a,b; Reyners 2011), including:

(1) The proximity and shallow depth of the earthquake, which is considered the primary factor. Geodetic inversions, using LiDAR constraints (Beavan et al. 2012) suggest that surface slip extended up to just below the surface, 3–4 km from Christchurch city centre.
(2) A high-stress drop for the earthquake was inferred by Fry & Gerstenberger (2011), who noted that the earthquake had an energy magnitude (M_E) of 6.75 compared with a moment magnitude (M_W) 6.2.
(3) Kinematic inversion of the strong motion data (Holden 2011) suggests that the direction of the rupture was northwestward and upwards, towards Christchurch city, potentially producing directivity effects (Holden 2011).
(4) Complex behaviour of the near-surface soil layers, described by Fry et al. (2011b), who noted that several records in Christchurch city show asymmetry in the acceleration records, similar to that previously observed in Japan by Aoi et al. (2008) and Yamada et al. (2009). Fry et al. (2011b) concluded that the soil's behaviour may have increased upward accelerations, in a so-called 'trampoline effect'.
(5) Wavefield modelling indicates that surface wave energy was modulated by the topography of the Banks Peninsula volcanics, with simulations yielding accelerations of over 2 *g* for some sites (Fry et al. 2011c).
(6) Site amplification effects associated with sedimentary basin reverberation effects likely increased ground accelerations at longer periods (Bradley & Cubrinovski 2011; Kaiser et al. 2011; Webb et al. 2011).

Prior to the February M_W6.2, earthquake there had been some post-Darfield seismicity south of Christchurch city, including a M_L5.0 event on 7 September 2010 (Figs 2, 3). Wave-field cross-correlation analysis has not yet confirmed the relationship of this earlier activity to the subsequent February earthquake in the vicinity.

Aftershocks between February and June 2011

Following the 22 February earthquake, aftershock activity increased across the Canterbury region (Figs 2, 3), with 87 events of $M_L > 4$: of those, nine were of $M_L > 5$, and of these four were on 22 February. Fig. 1d shows seismic activity on the northwest–southeast striking fault north of the Darfield mainshock, as well as aftershock activity south and southwest of Christchurch.

13 June 2011 Christchurch earthquake, and activity up to December 2011

On 13 June 2011, a M_W6.0 aftershock occurred near the suburb of Sumner, preceded an hour earlier by a M_W5.3 event: the relocated epicentres are <0.5 km apart (Table 1). Both of these events produced high accelerations in the southern and eastern suburbs (GeoNet 2011b; McVerry et al. 2011; Webb et al. 2011), as well as widespread liquefaction (Orense et al. 2011). MM values >8 were experienced in the southern and eastern suburbs of Christchurch (GeoNet 2011b), while peak ground accelerations in Christchurch reached 2 g in Sumner and 0.4 g in the central city (GeoNet 2011b; Webb et al. 2011). Vulnerable structures were further damaged in Christchurch city, and there was additional slope failure in the southern Port Hills. The extremely high accelerations at the Sumner station may have been accentuated by surface topography (Fry et al. 2011c).

The focal mechanism of the M_W6.0 event involved right-lateral strike-slip motion (Fig. 1) (Ristau 2008; Sibson et al. 2011), consistent with slip on either a north–northwest–south–southeast-striking or east–northeast–west–southwest-striking fault plane. Results from separate geodetic and strong motion inversions indicate that two distinct patches of slip occurred either on intersecting fault planes or on a single fault oriented north–northwest–south–southeast; the former interpretation is preferred by Beavan et al. (2012), while a single fault plane with an east–northeast–west–southwest orientation was preferred by Barnhart et al. (2011). The 13 June earthquakes were immediately followed by aftershock activity extending towards Port Levy and Pigeon Bay, along a distinct north–northwest–south–southeast trend (Fig. 2).

December 2011-January 2012 activity

An M_W5.8 earthquake occurred on 23 December 2011, c. 10 km east of Christchurch city centre, followed a few hours later by an M_W5.9 event, c. 15 km from the city centre (Figs. 2, 3). Following these events, more than 600 aftershocks (to the end of January 2012) have been located by GeoNet east of the inferred fault that produced the 13 June 2011 earthquake (Fig. 2). Moment tensor solutions for the largest events in this new sequence suggest reverse faulting mechanisms, with c. N45E–N60E strikes (GeoNet 2011a).

Prebbleton region

Throughout the Canterbury earthquake sequence, aftershocks have continued to occur between the eastern end of the Greendale Fault and the western end of the inferred Christchurch fault segments (Fig. 2). Fig. 6 shows the epicentres of aftershocks in the area between Lincoln and Hornby, as well as moment tensor solutions for two of the larger ($M_L>5$) events that occurred following the 22 February and 13 June 2011 earthquakes. One concern is that significant moment release has still not occurred in this region, in spite of continued aftershock activity (Beavan et al. 2012; Elliott et al., 2012). The sense of faulting suggested by the most recent $M>5$ events suggests a degree of north–northwest–south–southeast sinistral faulting, which would indicate short fault segments that may not be capable of hosting larger earthquakes, although right-lateral strike-slip faulting is likely towards the western edge of the Port Hills. Further relocation analysis is necessary before the complexity of the fault structure here can be discerned and the critical seismic behaviour of this region fully understood.

Conclusion

Over a period of many months, the Canterbury earthquake sequence developed from a relatively standard aftershock sequence following the M_W7.1 Darfield earthquake into a complex, long-lasting series of damaging earthquakes. This sequence will inform thinking of seismic hazard in New Zealand and internationally for decades to come. The earthquakes are characterised by complex ruptures and high accelerations. Of particular note is the destructive power of the M_W6.2 Christchurch earthquake of 22 February 2011, in which a number of factors, including the earthquake's proximity to the city and probable directivity effects, resulted in levels of damage higher than expected for the size of the earthquake. Understanding the reasons for the high levels of damage is vitally important for estimating the hazards posed by similar earthquakes near other New Zealand or international cities. A combination of aftershock studies and geodetic and strong motion source modelling utilising high-quality data is important for understanding the source mechanisms and rupture processes of the major earthquakes of the Canterbury sequence.

The presence of the GeoNet seismic network in the region, and throughout New Zealand, and the deployment of additional, temporary instruments, has provided an unparalleled data set that will enhance our understanding of this earthquake sequence and inform the earthquake hazard in similar (low strain rate) environments. To make best use of this data, the complete lifecycles of these earthquakes, their source mechanics and rupture processes, seismic path effects as modified by local crustal and basin structures, and the various site effects that enhanced the damaging potential of the earthquakes all need to be understood. Progress has already been made but much more is left to be done.

Acknowledgements

The authors acknowledge the extensive use of GeoNet data in many of the studies reported here, and the efforts of GeoNet and other

GNS Science staff in the collection and processing of the data. GeoNet is sponsored by the New Zealand Government through its agencies: Earthquake Commission (EQC), GNS Science and Land Information New Zealand (LINZ). Some of the figures were created using Generic Mapping Tools (GMT, Wessel & Smith 1991).

References

Abercrombie RE, Webb TH, Robinson R, McGinty PJ, Mori J, Beavan RJ 2000. The enigma of the Arthur's Pass, New Zealand, earthquake 1. Reconciling a variety of data for an unusual earthquake sequence. Journal of Geophysical Research 105: 16119–16137.

Aoi S, Kunugi T, Fujiwara H 2008. Trampoline effect in extreme ground motion. Science 322: 727–730. doi:10.1126/science.1163113

Bannister S 2011. Relocation analysis of the Christchurch city 'Boxing Day' earthquakes. GNS Science Consultancy report 2011/36. 9 p.

Bannister S, Fry B, Reyners M, Zhang H 2011. Fine-scale relocation of aftershocks of the M_w6.2 February 22nd Christchurch earthquake, using double-difference tomography. Seismological Research Letters 82: 839–845. doi:10.1785/gssrl.82.6.839

Barnhart WD, Willis MJ, Lohman RB, Melnonian AK 2011. InSAR and optical constraints on fault slip during the 2010–2011 New Zealand earthquake sequence. Seismological Research Letters 82: 815–823. doi:10.1785/gssrl.82.6.815

Beavan J, Fielding E, Motagh M, Samsonov S, Donnelly N 2011. Fault location and slip distribution of 22 February 2011 M_w 6.2 Christchurch, New Zealand, earthquake from geodetic data. Seismological Research Letters 82: 789–798. doi:10.1785/gssrl.82.6.789

Beavan J, Motagh M, Fielding E, Donnelly N, Collett D 2012. Fault slip models of the 2010–2011 Canterbury earthquakes from geodetic data, and observations of post-seismic ground deformation. New Zealand Journal Geology and Geophysics 55. doi:10.1080/00288306.2012.697472

Beavan RJ, Samsonov S, Motagh M, Wallace LM, Ellis SM, Palmer NG 2010. The Darfield (Canterbury) earthquake: geodetic observations and preliminary source model. Bulletin of the New Zealand Society for Earthquake Engineering 43(4): 228–235.

Bradley BA, Cubrinovski M 2011. Near-source strong ground motions observed in the 22 February 2011 Christchurch earthquake. Seismological Research Letters 82: 853–865. doi:10.1785/gssrl.82.6.853

Cousins WJ, McVerry GH 2010. Overview of strong-motion data from the Darfield earthquake. Bulletin of the New Zealand Society for Earthquake Engineering 43(4): 222–227.

Cubrinovski M, Bray JD, Taylor M, Giorgini S, Bradley B, Wotherspoon L, Zupan J 2011. Soil liquefaction effects in the central business district during the February 2011 Christchurch earthquake. Seismological Research Letters 82: 893–904. doi: 10.1785/gssrl.82.6.893

Dellow G, Yetton M, Massey C, Archibald G, Barrell D, Bell D, Bruce Z, Campbell A, Davies T, De Pascale G, Easton M, Forsyth J, Gibbons C, Glassey P, Grant H, Green R, Hancox G, Jongens R, Kingsbury P, Kupec J, MacFarlane D, McDowell B, McKelvey B, McMahon I, McPherson I, Molloy J, Muirson J, O'Halloran M, Perrin N, Price C, Read S, Traylen N, Van Dissen R, Villeneve M, Walsh I 2011. Landslides caused by the 22 February 2011 Christchurch Earthquake and management of landslide risk in the immediate aftermath. Bulletin of the New Zealand Society for Earthquake Engineering 44(4): 227–238.

Elliott JR, Nissen E, England PC, Jackson JA, Lamb S, Li Z, Oehlers M, Parsons BE. 2012 Slip in the 2010-2011 Canterbury earthquakes, New Zealand. Journal of Geophysical Research, 117, B03401. doi:10.1029/2011JB008868

Fry B, Benites R, Reyners M, Holden C, Kaiser A, Bannister S, Gerstenberger M, Williams C, Ristau J, Beavan J 2011a. Strong shaking in recent New Zealand earthquakes. Eos Transactions. American Geophysical Union 92: 349–360.

Fry B, Benites R, Kaiser A 2011b. The character of accelerations in the Christchurch M_w6.3 earthquake. Seismological Research Letters 82: 846–852. doi:10.1785/gssrl.82.6.846

Fry B, Benites RA, Francois-Holden C 2011c. The effect of near-field topography on the 2011 M_w6.3 Christchurch, NZ, earthquake. Abstract S52B-08 in: 2011 AGU Fall meeting, 4–9 December, San Francisco, California, USA. Washington, DC: American Geophysical Union.

Fry B, Gerstenberger MC 2011. Large apparent stresses from the Canterbury earthquakes of 2010 and 2011. Seismological Research Letters 82: 833–838. doi:10.1785/gssrl.82.6.834

GeoNet 2011a. GeoNet Moment Tensor Solution Database 2011. www.geonet.org.nz/resources/earthquake/ (accessed 14 February 2012).

GeoNet 2011b. http://www.geonet.org.nz/news/archives/2011/jun-2011-large-earthquakes-strike-south-east-of-christchurch.html (accessed 14 February 2012).

GeoNet 2011c. http://www.geonet.org.nz/resources/basic-data/waveform-data/ (accessed 25 May 2012).

Gledhill K, Ristau J, Reyners M, Fry B, Holden C 2011. The Darfield (Canterbury, New Zealand) M_w7.1 earthquake of September 2010: a preliminary seismological report. Seismological Research Letters 82: 378–386. doi:10.1785/gssrl.82.3.378

Holden C 2011. Kinematic source model of the 22 February 2011 M_w6.2 Christchurch earthquake using strong motion data, 2011. Seismological Research Letters 82: 783–788. doi:10.1785/gssrl.82.6.783

Holden C, Beavan J, Fry B, Reyners M, Ristau J, Van Dissen R, Villamor P, Quigley M 2011. Preliminary source model of the M_w7.1 Darfield earthquake from geological, geodetic and seismic data. In: Proceedings of the Ninth Pacific Conference on Earthquake Engineering, 14–16 April, paper no. 164, University of Auckland, Auckland, New Zealand, NZ: 9PCEE.

Kaiser A, Benites RA, Chung AI, Haines AJ, Cochran E, Fry B 2011. Estimating seismic site response in Christchurch city (New Zealand) from dense low-cost aftershock arrays. Extended abstract of the Fourth IASPEI/IAEE International Symposium on the Effects of Surface Geology on Seismic Motion, Santa Barbara, California 23–26 August. http://esg4.eri.ucsb.edu (accessed 25 May 2012).

McVerry GH, Gerstenberger MC, Rhoades DA 2011. Evaluation of the Z-factor and peak ground accelerations for Christchurch following the 13 June 2011 earthquake. GNS Science report 2011/45, 29p Lower Hutt, New Zealand, GNS Science.

Orense RP, Kiyota T, Yamada S, Curbinovski M, Hosno Y, Okamura M, Yasuda S 2011. Comparison of liquefaction features observed during the 2010 and 2011 Christchurch earthquakes. Seismological Research Letters 82: 905–918. doi:10.1785/gssrl.82.6.905

Quigley M, Villamor P, Furlong K, Beavan J, Van Dissen R, Litchfield N, Stahl T, Duffy B, Bilderback E, Noble D, Barrell D, Jongens R, Cox S 2010. Previously unknown fault shakes

New Zealand's South Island. EoS Transactions. American Geophysical Union 91: 469–488.

Quigley M, Van Dissen R, Litchfield N, Villamor P, Duffy B, Barrell D, Furlong K, Stahl T, Bilderback E, Noble D 2012. Surface rupture during the 2010 M_w7.1 Darfield (Canterbury) earthquake: Implications for fault rupture dynamics and seismic-hazard analysis. Geology 40: 55–58, doi:10.1130/G32528

Reyners M 2011. Lessons from the destructive Mw6.3 Christchurch, New Zealand, Earthquake. Seismological Research Letters 82(3): 371–372.

Ristau J. 2008. Implementation of routine regional moment tensor analysis in New Zealand. Seismological Research Letters 79: 400–415, doi: 10.1785/gssrl.79.3.400

Sibson R, Ghisetti F, Ristau J 2011. Stress control of an evolving strike-slip fault system during the 2010–2011 Canterbury, New Zealand, earthquake sequence. Seismological Research Letters 82: 824–832. doi:10.1785/gssrl.82.6.824

Syracuse E, Holt R, Savage M, Johnson J, Thurber C, Unglert K, Allan K, Karaliyadda S, Henderson M 2012. Hypocentres and anisotropy from the Darfield aftershock sequence: implications for fault geometry, age, and seismic property evolution, New Zealand Journal of Geology and Geophysics 55:

Van Dissen R, Barrell D, Licthfield N, Villamor P, Quigley M et al. 2011. Surface rupture displacement on the Greendale Fault during the M_w7.1 Darfield (Canterbury) earthquake, New Zealand, and its impact on man-made structures. Proceedings of the Ninth Pacific Conference on Earthquake Engineering, 14–16 April 2011, University of Auckland, Auckland, New Zealand: 9PCEE.

Villamor P, Litchfield N, Barrell D, Van Dissen R, Hornblow S, Quigley S, Levick L, Ries W, Duffy B, Begg J, Townsend D, Stahl T, Bilderback E, Noble D, Furlong K, Grant H 2012. Map of the 4 September, 2010, Greendale Fault surface rupture, Canterbury, New Zealand: application to land use planning. New Zealand Journal of Geology and Geophysics 55:

Webb TH (compiler), Bannister S, Beavan J, Berryman K, Brackley H, Cousings J, Fry B, Gerstenberger M et al. 2011. The Canterbury Earthquake Sequence and Implications for Seismic Design Levels, GNS Science Consultancy Report 2011/183. 88p Lower Hutt, New Zealand, GNS Science.

Wessel P, Smith WHE 1991. Free software helps map and display data. Eos, Transactions. American Geophysical Union 72: 441.

Yamada M, Mori J, Heaton T 2009. The slapdown phase in high acceleration records of large earthquakes. Seismological Research Letters 80: 559–564.

Zhang H, Thurber CH 2003. Double-difference tomography: the method and its application to the Hayward Fault, California. Bulletin Seismological Society of America 93: 1875–1889.